Available online at www.sciencedirect.com

SciVerse ScienceDirect

Geochimica et Cosmochimica Acta 75 (2011) 7552–7565

Geochimica et Cosmochimica Acta

www.elsevier.com/locate/gca

Hydrogen isotopes in individual alkenones from the Chesapeake Bay estuary

Valérie F. Schwab *, Julian P. Sachs

University of Washington, School of Oceanography, Box 355351, Seattle, WA 98195, USA

Received 21 February 2011; accepted in revised form 13 September 2011; available online 24 September 2011

Abstract

Hydrogen isotope ratios of individual alkenones from haptophyte algae were measured in suspended particles and surface sediment from the Chesapeake Bay (CB) estuary, eastern USA, in order to determine their relationship to water δD values and salinity. δD values of four alkenones ($MeC_{37:2}$, $MeC_{37:3}$, $EtC_{38:2}$, $EtC_{38:3}$) from particles and sediments were between $-165‰$ and $-221‰$ and increased linearly ($R^2 = 0.7$–0.9) with water δD values from the head to the mouth of the Bay. Individual alkenones were depleted in deuterium by 156–188‰ relative to water. The MeC_{37} alkenones were consistently enriched by ~12‰ relative to the EtC_{38} alkenones, and the di-unsaturated alkenones of both varieties were consistently enriched by ~20‰ relative to the tri-unsaturated alkenones. All of the increase in alkenone δD values could be accounted for by the water δD increase. Consequently, no net change in alkenone–water D/H fractionation occurred as a result of the salinity increase from 10 to 29. This observation is at odds with results from culture studies with alkenone-producing marine coccolithophorids, and from two field studies, one with a dinoflagellate sterol in the CB, and one with a wide variety of lipids in saline ponds on Christmas Island, that indicate a decline in D/H fractionation with increasing salinity. Why D/H fractionation in alkenones in the CB showed no dependence on salinity, while D/H fractionation in CB dinsoterol decreased by 1‰ per unit increase in salinity remains to be determined. Two hypotheses we consider to be valid are that (i) the assemblage of alkenone-producing haptophytes changes along the Bay and each species has a different sensitivity to salinity, such that no apparent trend in $\alpha_{alkenone-water}$ occurs along the salinity gradient, and (ii) greater osmoregulation capacity in coastal haptophytes may result in a diminished sensitivity of alkenone–water D/H fractionation to salinity changes.

1. INTRODUCTION

The hydrogen isotopic composition of algal lipids closely co-varies with the hydrogen isotope composition of the water in which the organisms grew (Sessions et al., 1999; Englebrecht and Sachs, 2005; Zhang and Sachs, 2007; Schwab and Sachs, 2009; Sachs and Schwab, 2011). Algal lipid D/H ratios in sediments have thus been increasingly used to reconstruct the water cycle in past environments (e.g., Sauer et al., 2001; Huang et al., 2002; Pahnke et al., 2007; Van der Meer et al., 2007, 2008; Sachs et al., 2009). However, beside the biosynthetic pathways (Sessions et al., 1999) and species-specific differences (Schouten et al., 2006; Zhang and Sachs, 2007), environmental parameters including temperature (Wolhowe et al., 2009; Zhang et al., 2009), nitrogen limited growth rate (Zhang et al., 2009), growth phase (Wolhowe et al., 2009) and salinity (Schouten et al., 2006; Sachse and Sachs, 2008; Sachs and Schwab, 2011) have been shown to influence hydrogen isotope fractionation during lipid synthesis by algae, potentially complicating paleohydrologic interpretations.

For instance, culture (Schouten et al., 2006) and field studies (Sachse and Sachs, 2008; Sachs and Schwab, 2011) demonstrated that increased salinity resulted in decreased D/H fractionation between environmental water and the

* Corresponding author. Present address: Max-Planck-Institute for Biogeochemistry, Hans-Knoell Strasse 10, 07745 Jena, Germany. Tel.: +49 3641 57 6105.

E-mail address: vschwab@bgc-jena.mpg.de (V.F. Schwab).

0016-7037/$ - see front matter © 2011 Elsevier Ltd. All rights reserved.
doi:10.1016/j.gca.2011.09.031

biosynthesized lipids. Paleosalinity and paleohydrologic reconstructions based on lipid δD values soon followed (Pahnke et al., 2007; Van der Meer et al., 2007, 2008; Sachs et al., 2009; Smittenberg et al., 2011). Internal cell water is the main donor of hydrogen atoms in all positions of the lipid chain (Duan et al., 2002; Baillif et al., 2009), and thus its hydrogen isotope composition is likely to be directly reflected in the biosynthesized lipids (Kreuzer-Martin et al., 2006). It has been thus proposed that the D-enrichment in algal lipids as salinity increases reflects progressive D-enrichment of internal cell water due to its continual enrichment as biosynthetic reactions draw D-depleted hydrogen from the internal water pool in combination with reduced exchange with external water (Sachse and Sachs, 2008; Sachs and Schwab, 2011). A refinement put forth by Sachs and Schwab (2011) is that turgor regulation via increased osmolyte production siphons off isotopically depleted H, leaving internal water used for lipid synthesis enriched in D. Nevertheless, the mechanisms controlling the sensitivity of lipid δD values to salinity are still being evaluated and a general theory to explain the phenomenon is lacking.

Prymnesiophyte algae are the unique producers of alkenones (Volkman et al., 1980; Marlowe et al., 1984). In the modern ocean, they are produced primarily by the species *Emiliania huxleyi* and *Gephyrocapsa oceanica*, (Marlowe et al., 1984, 1990; Conte et al., 1995; Volkman et al., 1995) while in coastal and lacustrine environments, the main producers are likely the species *Isochrysis galbana* and *Chrysotila lamellosa* (e.g., Volkman et al., 1988; Li et al., 1996; Thiel et al., 1997; Schulz et al., 2000; Chu et al., 2005; Sun et al., 2007).

Heretofore, the measurement of alkenone δD values has been performed on a mixture of the $C_{37:3}$ and $C_{37:2}$ alkenones owing to the inability to achieve adequate separation between the two compounds during gas chromatography (Englebrecht and Sachs, 2005; Schouten et al., 2006; Pahnke et al., 2007; Van der Meer et al., 2007, 2008). Separation techniques using column argentation chromatography or recently developed high-performance liquid chromatography-mass spectrometry (HPLC-MS) permit the purification of each individual alkenone for stable hydrogen isotope analyses based on the number of carbon atoms and double bonds (D'Andrea et al., 2007; Schwab and Sachs, 2009). Using the HPLC-MS technique, a systematic *ca.* 20‰ difference in the δD values of $C_{x:3}$ and $C_{x:2}$ alkenones (where $x = 37$ or 38) was measured in sediments and particles from a site in the CB estuary (Schwab and Sachs, 2009). An identical hydrogen isotopic offset between $C_{37:3}$ and $C_{37:2}$ alkenones ($\alpha_{C37:3\text{–}C37:2} = (\delta DC_{37:3}+1)/(\delta DC_{37:2}+1) = 0.97$) was recently measured in cultured *E. huxleyi* and *G. oceanica* harvested at different growth stages (Wolhowe et al., 2009). The similar isotopic offset between $C_{37:3}$ and $C_{37:2}$ alkenones in both studies, despite the likely presence of alkenone producers in the Chesapeake Bay (CB) other than *E. huxleyi* and *G. oceanica*, led Wolhowe et al. (2009) to propose that a simple isotopic mass balance calculation could be used to determine δD values for individual alkenones measured from total C_{37} alkenones (i.e., the combined $C_{37:2} + C_{37:3}$ alkenone peak eluting from a GC) without labor-intensive chemical separations.

To test the fidelity with which individual alkenones record water δD values and to evaluate the influence of salinity on D/H fractionation in alkenones, we measured the hydrogen isotope composition of these compounds along the salinity (10–29) and water δD (−37.6‰ to −10.6‰) gradient in the CB estuary in Maryland and Virginia, Eastern USA. The same set of samples was used by Sachs and Schwab (2011) to demonstrate that about half of the increase in dinosterol δD values along the CB resulted from increasing water δD values, and the other half from decreasing D/H fractionation as salinity increased. Our results are then used to test the hypothesis of Wolhowe et al. (2009) that the hydrogen isotope offsets between individual alkenones are constant in an estuarine environment characterized by large salinity variations.

2. MATERIALS AND METHODS

2.1. Geological setting and water chemistry

Located in the Mid-Atlantic region of North America, the CB is a N–S elongate (300 km), shallow (average depth 8.2 m) estuary with an axial channel that is 12–30 m deep (Fig. 1). Freshwater from the Susquehanna River at the head of the Bay supplies 48% of the total riverine flux of water to the CB and creates typical partially mixed estuarine circulation with an outflow of freshwater in the upper layers and an inflow of seawater at depth. A salinity gradient along the length of the CB, and as a function of depth is thus formed (e.g., Pritchard, 1967; Austin, 2004).

Multi-decadal time series of monthly physical, chemical and biological parameters in the CB are available on the website of the CB Monitoring Program http://www.chesapeakebay.net/data_waterquality). Salinity, water δD values, and water temperature at multiple depths along the N–S transect of the Bay in May 22–25, 2006 are published in Sachs and Schwab (2011). Nutrient, Chl *a* concentration and primary production at the same sampling locations are available on the CB Monitoring Program website. Briefly, surface (0–2 m) salinity and δD values increased from 0 to −56.8‰ (station CB1.1) at the head of the CB, where the Susquehanna River enters, to 28.9 and −11.4‰ (station CB7.4N) at the mouth of the Bay (Fig. 1). The water δD values, previously published in Sachs and Schwab (2011), were linearly correlated with salinity (increasing with depth and along the length of the estuary) according to the relationship $\delta D_{water} = 1.63 \pm 0.04 \times \text{Salinity} - 52.3 \pm 0.7$, $R^2 = 0.91$, with uncertainties represented as the standard errors of the slope and intercept of the regression. The observed relationship reflects fractionation due to evaporation toward more saline media and the mixing line between marine and freshwater (Craig, 1961; Craig and Gordon, 1965). Surface (0–2 m) water temperatures were between 14.9 and 20.1 °C. Lower temperatures occurred in the upper-bay (CB3.2) and lower-bay (CB7.4 N) and higher temperature in the mid-bay (CB6.2) (Fig. 1). A halocline and a thermocline were observed at all CB stations, with bottom waters as much as 15 saltier and 2 °C colder than surface waters. As a result, since freshwaters were depleted in deuterium by 50‰ relative to seawater, water δD values

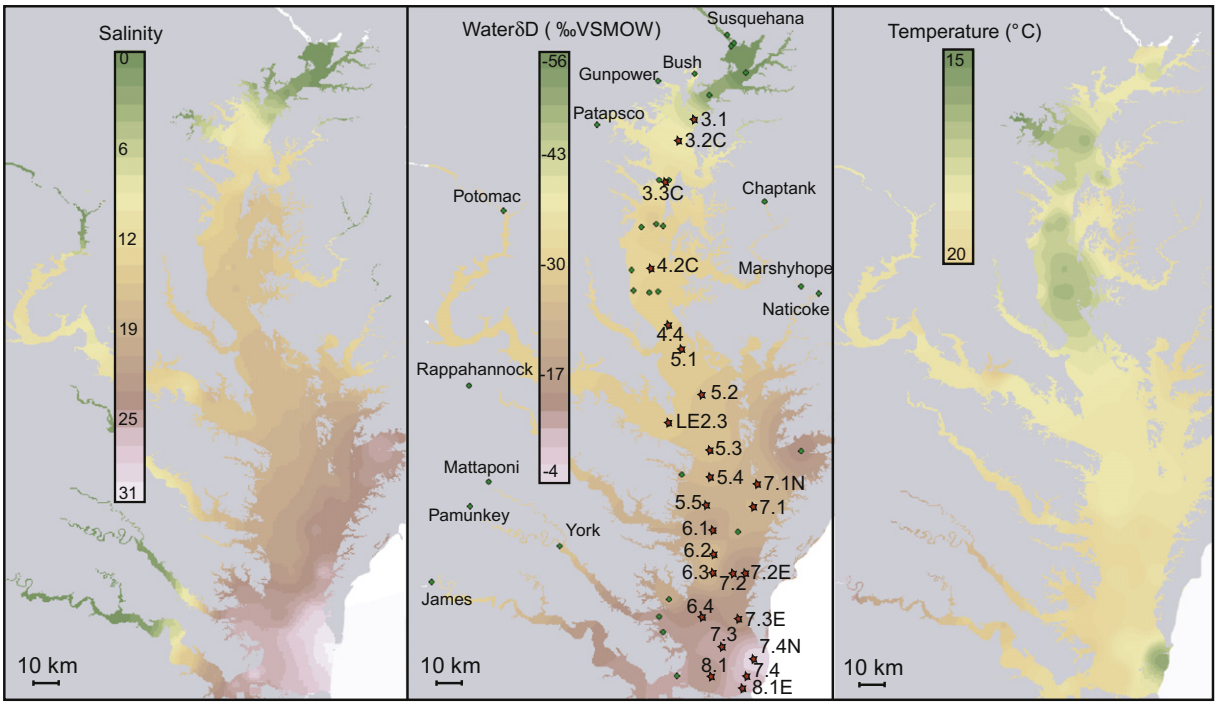

Fig. 1. Maps of the CB showing surface (0–2 m) water (a) salinity, (b) δD_{water} values and (c) temperature at sample locations (red stars green circles). The station locations from which surface sediment and suspended particle were taken for this study are shown with red stars. Maps were produced with ArcGIS Spatial Analyst, with inverse distance weighted output cell size of 0.001°, 131 salinity points, 105 water δD values, and 122 temperature points. Salinity and temperature data are from the CB monitoring program (http://www.chesapeakebay.net/data_waterquality). (For interpretation of the references to colour in this figure legend, the reader is referred to the web version of this article.)

increased with depth at all stations, with bottom waters as much as 15‰ heavier than surface waters. Total dissolved nitrogen and phosphate ranged from *ca*. 0.14 to 0.88 mg L^{-1} and from 5.0 to 23.6 μg L^{-1}, respectively, with both nutrients most abundant at the head of the Bay and least abundant at the mouth. In May 2006, surface Chl *a* concentrations were between 1.07 and 31.4 μg L^{-1}, with lowest values at the mouth (station CB7.4 N) of the Bay and highest values in the mid-Bay region. Maximum chlorophyll concentrations occurred at 3–5 m water depth throughout the Bay. Higher primary production in the mid-Bay resulted in hypoxic (1–30% saturation of dissolved oxygen) or anoxic bottom waters.

2.2. Water, particle and sediment sampling in the Chesapeake Bay

Surface sediment and suspended particles were collected at 26 of the CB Monitoring Program stations along the central axis of the Bay from the R/V Kerhin during May 22–25, 2006 (Fig. 1). Sample collection was timed to coincide with the haptophyte bloom that was expected to occur in late May, after peak runoff fluxes occurred (Mercer et al., 2005), and within two days of both the Maryland and Virginia Monitoring Program's monthly sampling of the Bay. The coordinates of each station and the detailed sampling procedure are published in Sachs and Schwab (2011). In brief, near surface sediments, collected with a grab sampler, were sub-sampled – typically at 0–2 and 0–10 cm – and subsequently frozen at −20 °C. Water and suspended particle samples were collected at multiple depths at each sampling site – typically 0–2, 2–4, 4–5, 14 and 30 m – by tubing attached to a conductivity–temperature–depth continuous profiling instrument and filtered through glass fiber filters immediately frozen at −20 °C. Water for hydrogen isotope analysis was collected with each filter and between stations. Salinity and temperature were continuously measured on board the vessel.

2.3. Coccolithophore identification

Samples were taken to determine coccolithophore taxonomic composition at each sample depth by vacuum filtering 1–2 L of water through cellulose nitrate and polycarbonates filters (0.45 μm pore size, 47 mm diameter). Each filter was rinsed with buffered water (63 mL of NH_4OH in 500 mL of distilled water) to remove salt, then dried at 40 °C. Filters were analyzed by polarized light microscopy at the University of Washington (Seattle, USA) and by scanning electron microscopy (SEM) at the University of Lausanne, Institute of Geology and paleontology (Switzerland).

2.4. Lipid extraction and pre-treatment

The detailed procedure for extracting and purifying alkenones is reported in Schwab and Sachs (2009). In brief, *n*-C_{37} alkane, 2-nonadecanone (C_{19}-ketone) and cholesterol

(Sigma–Aldrich) were added as internal standards to freeze-dried sediment and filters prior to extraction with an Automated Solvent Extractor (ASE-200, Dionex Corp., Sunnyvale, CA, USA). The solvent was removed under a stream of nitrogen using a Turbovap system (Caliper, Hopkinton, MA, USA). The extracts were separated with column chromatography on pre-combusted Al_2O_3 into four fractions: F1 was eluted with hexane/DCM (9:1, v/v) and contained hydrocarbons, F2 was eluted with hexane/DCM (1:1, v/v) and contained aromatic lipids and ketones (including alkenones), F3 was eluted with DCM/MeOH (1:1, v/v) and contained alcohols and F4 was eluted 100% MeOH and contained acids and polar lipids. Elemental sulphur was removed from F1 and F2 using activated Cu powder.

The alkenones and alkenoates contained in the F2 were identified by Gas Chromatography-Mass Spectrometry (GC–MS) using an Agilent (Santa Clara, CA, USA) 6890 N gas chromatograph equipped with an Agilent 5983 autosampler, a split-splitless injector operated in splitless mode, and a HP-5 ms column (30 m × 0.32 mm i.d. × 0.25 μm film thickness, Agilent) interfaced to an Agilent 5975 quadrupole mass selective detector (MSD). They were quantified with a Gas Chromatograph–Flame Ionization Detector (GC–FID). The Agilent 6890 GC was equipped with an Agilent 5983 autosampler and a programmable temperature vaporization inlet (PTV) operated in splitless mode. A 60 m Varian Chrompac CP-Sil 5 capillary column (0.32 mm × 0.25 μm) was used with helium as the carrier gas (1.6 mL/min).

2.5. Alkenone purification by HPLC-MS

Detailed methods for alkenones purification by HPLC are given in Schwab and Sachs, 2009. Briefly, an Agilent (Santa Clara, CA, USA) high performance liquid chromatograph (HPLC) 1100 series, equipped with an autoinjector, a quaternary pump, an integrated fraction collector, and Chemstation chromatography manager software was used. Typically, one injection of 100 μL of the concentrated F2 (alkenone) fraction was enough for subsequent hydrogen isotope analyses of each individual alkenone. A Prevail Cyano column (250 × 4.6 mm × 5μ; Alltech, Deerfield CA) maintained at 30 °C was used for separation. Compound classes were separated using an isocratic mixture of hexane and 4% DCM in hexane. Eluting compounds were identified in real-time with an Agilent 1100 SL mass spectrometer equipped with a multimode source operated in positive atmospheric pressure chemical ionization (APCI+) mode on *ca*. 2% of the total flow that was split from the eluent using an adjustable flow splitter (ASI, El Sobrante, CA, USA). A Waters (Milford, MA, USA) 510 pump was used to add a flow of 0.3 mL/min 2,2,4-trimethylpentane to the 2% split in order to supply sufficient solvent to the APCI source to achieve optimal ionization efficiency.

2.6. Hydrogen isotope analyses

Alkenones were quantified by comparing their integrated peak areas with that of the *n*-C_{37} standard using GC–FID operating at the same conditions previously described. The target compounds were dissolved in toluene to reach the adequate concentration (250–300 ng/μL of the individual alkenones) needed for sufficient signal intensity on the GC–IRMS system (Trace Ultra GC and DELTA V from Thermo Scientific, Waltham, MA, USA). The GC was equipped with a split-splitless injector operated in splitless mode at 300 °C, a TRIPLUS autosampler (Thermo Scientific, Waltham, MA, USA), and a DB-5ms capillary column (60 m × 0.32 mm × 0.25 μm, Agilent). Helium was used as the carrier gas at a constant flow of 1 mL/min.

Instrument performance and the H_3^+ factor were determined on a daily basis using a tank of H_2 reference gas (Sessions et al., 2001) and a mixture of *n*-alkanes (*n*-C_{14} to *n*-C_{44}) of known isotopic composition. Hydrogen isotopic composition of *n*-C_{14} to *n*-C_{36} *n*-alkane was determined off-line using a thermochemical elemental analyzer (TC/EA) (Thermo-Fisher, Bremen, Germany) interfaced to the DELTA V PLUS irMS system via a Conflo III combustion interface (Thermo-Fisher, Bremen, Germany). The *n*-C_{38}, *n*-C_{41} and *n*-C_{44} standards used for δD corrections and added to the *n*-alkane mixture for H_3^+ factor calculation were purchased from A. Schimmelmann, (Indiana University, Bloomington, Indiana). The average offset between GC-irMS δD values and those determined off-line was 3.9‰ ($n = 3630$, 165 runs with 22 peaks). The H_3^+ factor was lower than four and stable during the measurements reported here. The precision of alkenone δD measurements, as determined by the pooled standard deviation, $S_p = \sqrt{\frac{\sum_{i=1}^{k}((n_i-1)s_i^2)}{\sum_{i=1}^{k}(n_i-1)}}$ of 363 analyses of 119 samples, seven of which were measured in quadruple, 111 of which were measured in triplicate and one in duplicate, was 1.3‰.

3. RESULTS

3.1. Alkenone producers in the Chesapeake Bay

No evidence of calcified haptophyte species, such as the common marine coccolithophorids *E. huxleyi* and *G. oceanica*, was found in 10 samples investigated by light microscopy or two samples investigated by SEM despite both those species having been reported in the Bay (Marshall, 1994; Marshall et al., 2005). Although the two samples investigated by SEM (station CB4.4 and station CB7.4) do not represent a comprehensive set of all sites in the Bay, they did contain substantial concentrations of alkenones. Light microscopy revealed the occurrence of uncalcified spherical cells in all samples tentatively identified as *I. galbana* or *C. lamellosa*. Both of those species have been identified in the Bay (Marshall, 1994; Marshall et al., 2005) and are known to produce alkenones (Versteegh et al., 2001; Sun et al., 2007). However, since *E. huxleyi* and *G. oceanica* may lose their coccoliths under certain environmental conditions and/or phases of growth (Green et al., 1996; Paasche, 2002), we cannot definitively exclude their presence in the CB. Doing so would require DNA analyses

since taxonomic differentiations on naked cells are nearly impossible by SEM (Coolen et al., 2004).

3.2. Alkenone distributions along the bay

Alkenones were detected throughout the Bay in suspended particles from a variety of depths (Electronic annex Table EA-1) and in surface sediments (Electronic annex Table EA-3) collected between station CB3.1 and CB7.4N at salinities ranging from 3.7 to 30.9 (Fig. 1). Alkenone concentrations in water ranged from 0.01 to 0.36 μg L^{-1} in the Upper-Bay, from 0.06 to 2.1 μg L^{-1} in the Mid-Bay and from 0.04 to 1.3 μg L^{-1} in the Lower-Bay (Table EA-1). Converted to mass of suspended matter, alkenone concentration were between 0.4–23.6 μg g^{-1} in the Upper-Bay, 1.8–271.4 μg g^{-1} in the Mid-Bay and 3.2–86.3 μg g^{-1} in the Lower-Bay (Table EA-1). At individual stations highest alkenone concentrations usually occurred between 1 and 5 m, close to the depth of maximum of Chl *a* concentration. Alkenone concentrations in sediments averaged a factor of four lower than in filters, but tracked concentrations in the overlying water, with higher concentrations of 42.5 μg g^{-1} at station CB6.1, and lower concentrations of 0.8–0.6 μg g^{-1} at station CB3.3E and CB7.4 in the Lower- and Upper-Bay, respectively (Table EA-3).

All particulate and sediment samples were characterized by similar alkenone distribution patterns to those shown in Schwab and Sachs (2009), with a predominance of methyl C_{37} alkenones over ethyl C_{38} alkenones, a higher relative concentration of tri- over di- and tetraunsaturated C_{37} and C_{38} alkenones, a small proportion of C_{39} alkenones, and trace amounts of tetraunsaturated C_{38} and C_{40} alkenones (Fig. 2). Only methyl and ethyl $C_{36:3}$ and $C_{36:2}$ alkenoates were detected, with ethyl $C_{36:2}$ alkenoate predominating. A distinct characteristic of all alkenone distributions was the lack of C_{38} methyl alkenones.

The relative abundance of the tetra-unsaturated C_{37} alkenone, expressed as $\%C_{37:4} = C_{37:4}/(C_{37:4} + C_{37:3} + C_{37:2})$ (Marlowe et al., 1984), was between 2.3–9.5% in particles (Table EA-2) and 2.0–10.5% in surface sediments (Table EA-3), and increased with salinity along the N–S transect of the Bay and with depth (Fig. 3A). For instance, between 0.5–3 m and 23 m at the station CB3.3C, salinity increased from 10.2 to 20.7 and $\%C_{37:4}$ increased 3.5 and 5.7 (Fig 3A).

The relative abundance of C_{37} alkenones relative to C_{38} alkenones, expressed as $C_{37}/C_{38} = (C_{37:3} + C_{37:2})/(C_{38:3} + C_{38:2})$ (Marlowe et al., 1984) was between 1.2–4.5 in particles and 1.1–2.1 in sediments (Tables EA-2 and EA-3). Samples between stations CB3.1 and CB7.4 indicated a decrease of C_{37}/C_{38} (from 3.1 to 1.2) as salinity increased from 3.7 to 28.9 along the N–S transect of the Bay and with depth (Fig. 3B). A different trend was observed at station CB7.4N, where two particle samples collected at 5 and 11 m displayed much higher C_{37}/C_{38} ratios of 4.2 and 4.5, respectively, in the salinity range 29.7 at 5 m to 30.9 at 11 m. No correlation between either $\%C_{37:4}$ or C_{37}/C_{38} with water temperature or nutrient concentration was observed.

In particles and sediments, alkenone indices such as $U^{K}_{37} = C_{37:2} - C_{37:4}/C_{37:2} + C_{37:3} + C_{37:4}$ (Brassell et al., 1986) and $U^{K'}_{37} = C_{37:2}/C_{37:2} + C_{37:3}$ (Prahl and Wakeham, 1987) displayed large variations throughout the Bay. Contrary to an earlier report by Mercer et al. (2005) U^{K}_{37} and $U^{K'}_{37}$ in particles and surface sediment showed no correlation with temperature (e.g. Fig. 4). In suspended particles, U^{K}_{37}

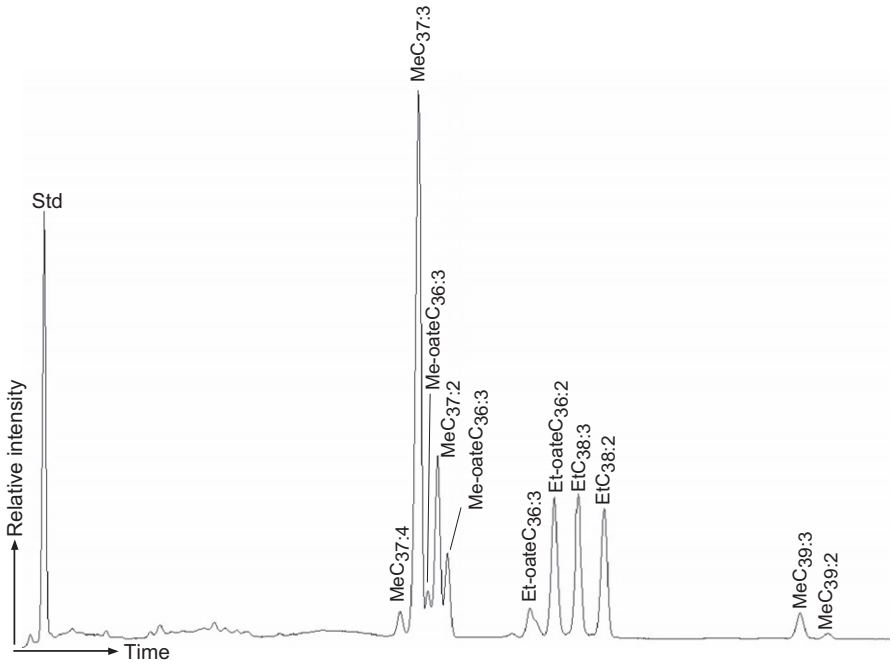

Fig. 2. Partial gas chromatogram showing representative alkenone distribution in surface sediments of the CB; with Me and Et being Methyl and Ethyl alkenone, respectively and Me-and Et-oate being Methyl and Ethyl alkenoate, respectively.

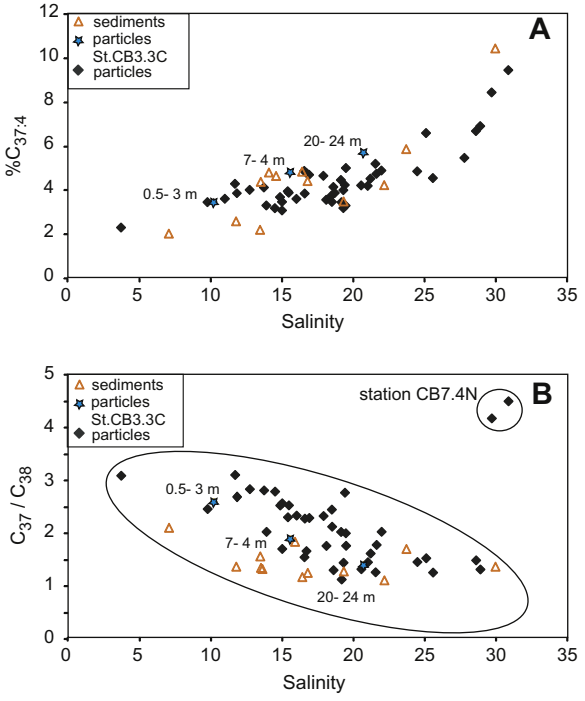

Fig. 3. (A) Plot showing variations of $\%C_{37:4}$ ratios versus salinity in water particle (black lozenge dots) and sediment (yellow triangle dots) samples. (B) Plot showing variations of C_{37}/C_{38} ratios versus salinity in water particle (black lozenge dots) and sediment (yellow triangle dots) samples. The blue star dots show the variation of these former ratios in water particle samples collected at 0.5–3, 7–4 and 20–24 m in station CB3.3C. (For interpretation of the references to colour in this figure legend, the reader is referred to the web version of this article.)

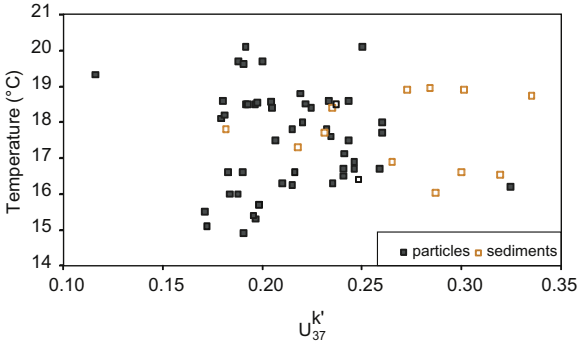

Fig. 4. Plot showing variations of $U_{37}^{K'}$ versus measured surface temperature in water particle (black dots) and sediment (yellow dots) samples. (For interpretation of the references to colour in this figure legend, the reader is referred to the web version of this article.)

and $U_{37}^{K'}$ ranged from 0.06 to 0.22 and from 0.12 to 0.26, respectively (Table EA-2). In sediment, U_{37}^{K} and $U_{37}^{K'}$ ranged from 0.12 to 0.28 and from 0.18 to 0.33, respectively (Table EA-3). Water surface temperatures derived from the relationship $U_{37}^{K'} = 0.034T + 0.039$ (Prahl et al., 1988) were between 2.3–8.4 °C in particles (Table EA-1) and 4.2–8.7 °C in sediment (Table EA-3), all 7.7–17.1 °C (average 12.4 °C) colder than the measured water temperature. Improved estimates of the water temperature were obtained using the alkenone temperature calibrations $U_{37}^{K} = 0.0377T–0.5992$ (Sun et al., 2007) and $U_{37}^{K'} = 0.016T–0.0607$ (Versteegh et al., 2001) calibrated with *C. lamellosa* and *I. galbana*, respectively. Applying the *C. lamellosa* calibration, $U_{37}^{K'}$-derived water temperatures were between 17.6–21.7 °C in particles and 15.9–23.3 °C in sediments, which together averaged 2.7 ± 1.9 °C warmer than measured temperatures. Applying the *I. galbana* temperature calibration, $U_{37}^{K'}$-derived water temperatures were between 11.0–24.1 °C in particles and 15.1–24.7 °C in sediments, on average just 0.3 ± 2.9 °C colder than measured temperatures (Tables EA-1 and EA-3).

3.3. Alkenone δD values

Alkenone δD values were measured in sediment and particle samples with sufficient alkenone abundance, which in this study was approximately greater than 1 μg of the total lipid extract. Such abundances occurred between stations CB3.3C and CB7.4N where surface salinities were between 10–29 and water δD values were between −37.6‰ and −10.6‰. The δD values of individual alkenones ($MeC_{37:2}$; $MeC_{37:3}$; $EtC_{38:2}$; $EtC_{38:3}$) in suspended particles collected at different depths are shown in Table EA-4A along with the associated water δD, salinity and temperature values. Individual alkenone δD values from surface sediments (0–10 cm) are listed in Table EA-4B along with the salinity and water δD values from water depths of 2–5 m, where highest alkenone concentrations occurred (Table-EA-1).

δD values of alkenones from particles and sediments were between −207‰ to −182‰ for $MeC_{37:3}$, −185‰ to −165‰ for $MeC_{37:2}$, −221‰ to −196‰ for $EtC_{38:3}$, and −197‰ to −175‰ for $EtC_{38:2}$. No significant difference in the δD value of individual alkenones was observed between surface sediments and particles in the overlying water column. Individual alkenones were depleted in deuterium relative to water by an amount that was lipid-specific but relatively constant throughout the Bay. That amount was -177 ± 2.9‰ ($n = 35$) for $MeC_{37:3}$, -156 ± 3.2‰ ($n = 25$) for $MeC_{37:2}$, -188 ± 3.2‰ ($n = 28$) for $EtC_{38:3}$, and -168 ± 3.0‰ ($n = 30$) for $EtC_{38:2}$. These isotopic fractionations are expressed as $\varepsilon_{alkenone–water}$ values ($\varepsilon_{alkenone–water} = (\alpha_{alkenone–water} - 1) = [(\delta D_{alkenone} + 1)/(\delta D_{water} + 1) - 1]$ in Tables EA-4A and EA-4B.

Particulate and sedimentary alkenone δD values were linearly correlated with water δD values with R^2 values of 0.8–0.9 in particles and 0.7–0.9 in sediments (Table 1, Fig. 5A). As salinity was linearly correlated with water δD values (Sachs and Schwab, 2011), alkenone δD values were linearly correlated with salinity with R^2 values of 0.6–0.8 in particles and 0.8 in sediments (Table 1, Fig. 5B). Linear regression analyses of $\delta D_{alkenone} = \alpha_{slope}\delta D_{water} + \varepsilon_{intercept}$ relationships indicated similar slopes (α_{slope}) of 0.703 ± 0.07 ($n = 8$) for each type of alkenone in both particles and sediments. But, intercepts ($\varepsilon_{intercept}$) differed for each type of alkenone: −178‰ for

Table 1
Equations of the relationships between individual alkenones and water δD values, individual alkenone δD values and salinity, and $\alpha_{alkenone-water}$ and salinity in sediment and water particle samples. Relationships between coeluting alkenones and water δD from others studies are shown for comparison.

Compound	Type of samples	Equation line δD alkenone versus δD water and salinity	R^2	n	$\alpha_{alkenone-water}$ − slope	$\alpha_{alkenone-water}$ − intercept	Equation line $\alpha_{alkenone-water}$ versus salinity	R^2	n
$MeC_{37:3}$	Sediment	$\delta D_{alk} = 0.793\delta D_{water} - 177.2^{*}$	0.79	16	0.793	0.823	$\alpha_{alkenone-water} = 0.0000salinity + 0.824$	0.1	16
$MeC_{37:3}$	Filter	$\delta D_{alk} = 0.710\delta D_{water} - 179.5^{*}$	0.85	19	0.710	0.821	$\alpha_{alkenone-water} = -0.0002salinity + 0.827$	0.2	19
$MeC_{37:2}$	Sediment	$\delta D_{alk} = 0.585\delta D_{water} - 164.4^{*}$	0.72	11	0.585	0.836	$\alpha_{alkenone-water} = -0.0004salinity + 0.849$	0.5	11
$MeC_{37:2}$	Filter	$\delta D_{alk} = 0.701\delta D_{water} - 158.0^{*}$	0.87	16	0.701	0.842	$\alpha_{alkenone-water} = -0.0002salinity + 0.848^{*}$	0.1	16
$EtC_{38:3}$	Sediment	$\delta D_{alk} = 0.776\delta D_{water} - 190.6^{*}$	0.85	13	0.776	0.809	$\alpha_{alkenone-water} = -0.0001salinity + 0.812$	0.1	13
$EtC_{38:3}$	Filter	$\delta D_{alk} = 0.618\delta D_{water} - 191.1^{*}$	0.77	15	0.618	0.809	$\alpha_{alkenone-water} = -0.0002salinity + 0.817^{*}$	0.2	15
$EtC_{38:2}$	Sediment	$\delta D_{alk} = 0.680\delta D_{water} - 172.5^{*}$	0.78	14	0.680	0.828	$\alpha_{alkenone-water} = -0.0003salinity + 0.835$	0.2	14
$EtC_{38:2}$	Filter	$\delta D_{alk} = 0.761\delta D_{water} - 168.3^{*}$	0.83	16	0.761	0.832	$\alpha_{alkenone-water} = -0.0001salinity + 0.834^{*}$	0.1	16
$MeC_{37:3}$	Sediment	$\delta D_{alk} = 1.307sal - 218.3^{*}$	0.81	16	1.307	0.782			
$MeC_{37:3}$	Filter	$\delta D_{alk} = 0.915sal - 212.3^{*}$	0.63	19	0.915	0.788			
$MeC_{37:2}$	Sediment	$\delta D_{alk} = 0.900sal - 193.9^{*}$	0.85	11	0.900	0.806			
$MeC_{37:2}$	Filter	$\delta D_{alk} = 0.958sal - 192.0^{*}$	0.65	16	0.958	0.808			
$EtC_{38:3}$	Sediment	$\delta D_{alk} = 1.121sal - 228.0^{*}$	0.78	13	1.121	0.772			
$EtC_{38:3}$	Filter	$\delta D_{alk} = 0.911sal - 221.1^{*}$	0.78	15	0.911	0.779			
$EtC_{38:2}$	Sediment	$\delta D_{alk} = 1.102sal - 207.3^{*}$	0.85	14	1.102	0.793			
$EtC_{38:2}$	Filter	$\delta D_{alk} = 1.172sal - 206.3^{*}$	0.83	16	1.172	0.794			
$MeC_{37:3} + MeC_{37:2}$		$\delta D_{alk} = 0.732\delta D_{water} - 225.2$	0.99	5	0.732	0.775	From Englebrecht and Sachs (2005)		
$EtC_{38:3} + EtC_{38:2}$		$\delta D_{alk} = 0.745\delta D_{water} - 232.8$	0.99	5	0.745	0.767	From Englebrecht and Sachs (2005)		
$MeC_{37:3} + MeC_{37:2}$		$\delta D_{alk} = 2.6\delta D_{water} - 215$	0.85	11	2.600	0.785	From Schouten et al. (2006) (*E.huleyi*)		
$MeC_{37:3} + MeC_{37:2}$		$\delta D_{alk} = 2.9\delta D_{water} - 242$	0.76	6	2.900	0.758	From Schouten et al. (2006) (*G. oceanica*)		

$\alpha_{alkenone-water}$ − intercept $= 1 - (-\epsilon/1000)$.
* =equation in a confidence level of at least 95%.

$MeC_{37:3}$, −161‰ for $MeC_{37:2}$, −191‰ for $EtC_{38:3}$, and −170‰ for $EtC_{38:2}$. Calculation of the fractionation factor using the intercept ($\alpha_{intercept} = 1 - (-\varepsilon_{intercept}/1)$) gave

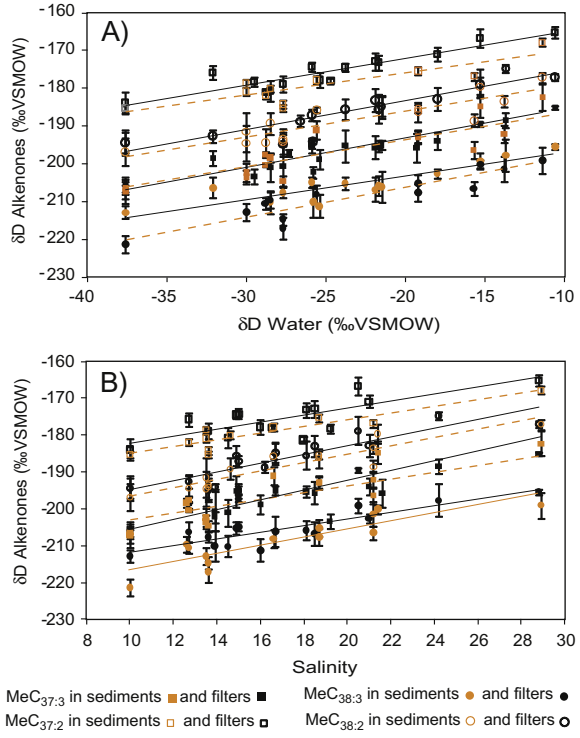

Fig. 5. CB individual alkenones δD values in water particle (black dots) and sediment (yellow dots) samples plotted against water δD values (A) and salinity (B). Equation lines and R^2 of these relationships are listed in Table 1. (For interpretation of the references to colour in this figure legend, the reader is referred to the web version of this article.)

Table 2
D/H fractionation ratios between the different alkenones and water ($\alpha C_{3x:y\text{–water}}$) and between the different alkenones ($\alpha_{C3x:y\text{–}C3x:y}$) in water particles and sediments.

Ratios	Sample type	D/H fractionation	Number of samples
$\alpha C_{37:3\text{–water}}$	Filter	0.823 ± 0.002	19
$\alpha C_{37:3\text{–water}}$	Sediment	0.823 ± 0.003	16
$\alpha C_{37:2\text{–water}}$	Filter	0.846 ± 0.002	16
$\alpha C_{37:2\text{–water}}$	Sediment	0.842 ± 0.003	11
$\alpha C_{38:3\text{–water}}$	Filter	0.814 ± 0.002	15
$\alpha C_{38:3\text{–water}}$	Sediment	0.810 ± 0.003	13
$\alpha C_{38:2\text{–water}}$	Filter	0.833 ± 0.002	16
$\alpha C_{38:2\text{–water}}$	Sediment	0.831 ± 0.003	14
$\alpha_{C37:3\text{–}C37:2}$	Filter	0.973 ± 0.02	14
$\alpha_{C37:3\text{–}C37:2}$	Sediment	0.974 ± 0.04	9
$\alpha_{C37:2\text{–}C38:2}$	Filter	1.015 ± 0.03	12
$\alpha_{C37:2\text{–}C38:2}$	Sediment	1.014 ± 0.08	10
$\alpha_{C38:3\text{–}C38:2}$	Filter	0.977 ± 0.04	14
$\alpha_{C38:3\text{–}C38:2}$	Sediment	0.969 ± 0.14	13
$\alpha_{C37:3\text{–}C38:3}$	Filter	0.992 ± 0.08	15
$\alpha_{C37:3\text{–}C38:3}$	Sediment	0.981 ± 0.09	10

$\alpha C_{3x:y\text{–water}} = (1 + \delta D_{alk})/(1 + \delta D_{water})$ and $\alpha_{C3x:y\text{–}C3x:y} = (C_{3x:y} + 1)/(C_{3x:y+1})$ with $x = 7$ or 8 and $y = 2$ or 3.

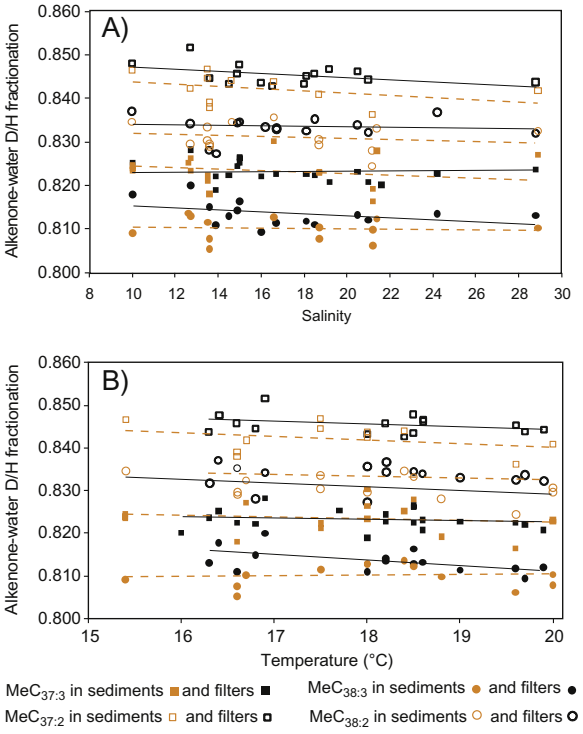

Fig. 6. CB $\alpha_{alkenones\text{–water}}$ in water particle (black dots) and sediment (yellow dots) samples plotted against salinity (A) and temperature (B). Equation lines and R^2 of these relationships are listed in Table 1. (For interpretation of the references to colour in this figure legend, the reader is referred to the web version of this article.)

values close to the fractionation factors derived from the slope (α_{slope}), with $\alpha_{intercept}$ on average 0.1 higher than α_{slope} (Table 1). The D/H fractionation between the different alkenones and water ($\alpha_{alkenone\text{–water}} = (1 + \delta D_{alk})/(1 + \delta D_{water})$ was nearly constant along the salinity gradient of the Bay (Table 2, Fig. 6A). Hydrogen isotopic offsets between di- and tri-unsaturated C_{37} and C_{38} alkenones ($\alpha_{C37:2\ -\ C37:3}$ and $\alpha_{C38:2\ -\ C38:3}$, where $\alpha_{C37:x\ -\ C38:x} = (C_{37:x} + 1)/(C_{37:x} + 1)$ with $x = 2$ or 3) and between C_{37} and C_{38} alkenones ($\alpha_{C37:2\ -\ C38:2}$ and $\alpha_{C37:3\ -\ C38:3}$), where $\alpha C3x:3\ -\ C3x:2 = (C_{3x:3} + 1)/(C_{3x:2} + 1)$ with $x = 7$ or 8) were similar in all particulate and sediment samples collected in the CB (Table 2 and Electronic annex Tables EA-5A and EA-5B).

4. DISCUSSION

4.1. Alkenones and alkenone-producing haptophytes in the Chesapeake Bay

All particulate and sediment samples were characterized by low abundances of C_{38} methyl alkenones and the $C_{38:4}$ alkenone, implying minor contributions of alkenones from oceanic haptophyte species such as *E. huxleyi* and *G. oceanica* (Marlowe et al., 1984; Rontani et al., 2004) relative to those favoring fresh or brackish water (Marlowe et al., 1984; Volkman et al., 1995; Li et al., 1996; Thiel et al., 1997; Schulz et al., 2000; Sun et al., 2007). Similar

distributions of alkenones have been reported in marginal and lacustrine environments characterized by uncalcified haptophytes such as *C. lamellosa*, *I. galbana* and *Chromulina* sp. (Cranwell, 1985; Volkman et al., 1988; Versteegh et al., 2001; Sun et al., 2007). The light microscopic and SEM-based identification of uncalcified haptophyte cells in our samples and reports of *C. lamellosa* and *I. galbana* in the Bay (Marshall, 1994; Marshall et al., 2005) support the notion that these species contributed substantially to the production of alkenones in our samples. The haptophyte bloom was reported to occur in late spring and to account for the bulk of the alkenone production during the year in the CB (Mercer et al., 2005). Therefore, alkenone indices in surface sediments likely represent long-term (i.e., 1–10 years, based on a linear sedimentation rate of 0.1–1 cm yr^{-1} (Colman and Bratton, 2003; Cronin et al., 2010) averaged surface conditions occurring in late spring when runoff of D-depleted freshwater into the CB is high.

4.1.1. C_{37}/C_{38} and $\%C_{37:4}$

The ratio of C_{37}/C_{38} alkenones in the CB was 1.2–4.5 in particles and 1.1–2.4 in sediments, averaging 2.2 (Tables EA-2 and EA-3). Open ocean ratios are typically between 0.5 and 1.5 (Conte et al., 1998; Chu et al., 2005), similar to those found in the most common marine alkenone producers, *E. huxleyi* (0.86–2.16, mean of 1.16 (Conte et al., 1994)) and *G. oceanica* (0.59–0.81, mean of 0.7 (Volkman et al., 1995)). Coastal haptophytes tend to have higher C_{37}/C_{38} ratios, such as *C. lamellosa* (1.4–9.5, mean of 5.6 (Prahl et al., 1988)) and *I. galbana* (5.4–15.1, mean of 10.9 (Marlowe et al., 1984)), and values in excess of two have been reported in the Baltic Sea (Schulz et al., 2000) and some lacustrine environments (Cranwell, 1985; Thiel et al., 1997; Chu et al., 2005 and references therein) and attributed to alkenone production by species similar to *C. lamellosa* and *I. galbana*. We thus tentatively attribute average C_{37}/C_{38} ratios of 2.2 in the CB to substantial alkenone production by coastal haptophytes such as *C. lamellosa* and *I. galbana*, noting, however, that Theroux et al. (2010) suggested that C_{37}/C_{38} ratios better reflect algal growth status than species identity.

Relatively high concentrations of $C_{37:4}$ compared to $(C_{37:3} + C_{37:2})$ have been reported in low salinity marginal, coastal and estuarine environments (Rosell-Melé, 1998; Volkman et al., 1988; Schulz et al., 2000; Blanz et al., 2005; Mercer et al., 2005), while very high $\%C_{37:4}$ values of up to 95% have been found in lacustrine sediments (Cranwell, 1985; Chu et al., 2005 and references therein). It was thus proposed that $\%C_{37:4}$ values could be used as a paleosalinity or water mass proxy (Rosell-Melé, 1998; Schulz et al., 2000; Blanz et al., 2005). Furthermore, analysis of fossil DNA from sediments in hypersaline Ace Lake, Antarctica, showed that higher $\%C_{37:4}$ values are correlated with higher relative abundance of freshwater versus oceanic haptophyte phylotypes (Coolen et al., 2004).

According to these studies, high values of both C_{37}/C_{38} and $\%C_{37:4}$ are commonly associated with a predominance of freshwater and coastal haptophytes (Chu et al., 2005 and references therein). In the CB, a negative correlation between C_{37}/C_{38} and salinity (Fig. 3B) supports these observations. But a positive correlation between $\%C_{37:4}$ and salinity (Fig. 3A) is inconsistent with these results. These opposite trends imply that physiological and/or species changes in alkenone producers along the salinity gradient in the CB differ from those in other settings. Furthermore, Toney et al. (2010) found a complete absence of $C_{37:4}$ in some lacustrine settings that was attributed to the presence of unidentified freshwater alkenone producers. Higher contributions of similar species in the upper reaches (i.e., low salinity region) of the CB may be an alternative explanation for the uncommon trend of $\%C_{37:4}$ as a function of salinity.

4.1.2. $U^{K'}_{37}$ and U^{K}_{37} temperature indices

A vast amount of literature demonstrates the high fidelity with which the alkenone unsaturation ratio $U^{K'}_{37}$ co-varies with sea surface temperature (SST) in the ocean, and the suitability of a single global temperature calibration equation ($U^{K'}_{37} = 0.034T + 0.039$) (see review by Herbert (2001)). When *E. huxleyi* and *G. oceanica* are not the predominant alkenone producers very different temperature calibrations have been reported (e.g., Rosell-Melé, 1998; Schulz et al., 2000; Chu et al., 2005; Mercer et al., 2005), making alkenone-based SST reconstructions uncertain when the identity of alkenone producers is unknown. Reconstructed SSTs in the CB are closer to measured values when temperature calibrations for *I. galbana* (Versteegh et al., 2001) and *C. lamellose* (Sun et al., 2007) are used than when marine (Prahl et al., 1988) calibrations are used. This provides further evidence that these coastal species may predominate the assemblage of alkenone-producing haptophytes in the CB. The absence of correlation between U^{K}_{37} or $U^{K'}_{37}$ and SSTs (e.g. Fig. 4) may be due to variations in the growth phase or the assemblage of alkenone producers along the CB (see discussion below), both of which are known to influence U^{K}_{37} and $U^{K'}_{37}$ (e.g., Conte et al., 1994; Mercer et al., 2005; Toney et al., 2010), or alternatively to the small range of temperature observed during sampling.

4.2. CB alkenone δD values

The CB estuary provides an ideal setting to evaluate (i) the fidelity with which alkenone lipids record the hydrogen isotopic composition of water and (ii) the influence of salinity on D/H fractionation in those lipids, because ample alkenone concentrations exist for hydrogen isotope analyses over a ~200 km estuary in water spanning a δD range of 27‰ (−38‰ to −11‰) and a salinity range of 19 (10.0–28.8). Below we first discuss the relationship between water δD values and δD values in four different alkenones from CB particles and surface sediments, demonstrating that these lipids faithfully track the isotopic composition of water. A discussion of the invariant D/H fractionation between water and alkenones along the salinity gradient of 19 follows.

4.2.1. Relationship between alkenone and water δD values

Our sampling in late May was timed to occur during the maximum of the annual alkenone production that occurs in late spring when runoff of D-depleted freshwater into the

CB is at a maximum (Mercer et al., 2005). Therefore, the similitude of alkenone δD values in particulate and sediment samples suggest that alkenone δD values in sediment record long-term (i.e., 1–10 years, based on a linear sedimentation rate of 0.1–1 cm yr^{-1} (Colman and Bratton, 2003; Cronin et al., 2010) average surface D-depleted water by late spring freshwater runoff.

Different intercept (ε) but similar slope (α) values for each of the four alkenones in the equation $\delta D_{alkenone} = \alpha\delta D_{water} + \varepsilon$ indicate that, while different for each of the four alkenones, the magnitude of lipid-water D/H fractionation for each remains constant along the length of the CB (Table 1). Furthermore, previous culture experiments of the oceanic haptophytes *E. huxleyi* and *G. oceanica* showed higher alkenone-water D/H fractionation of 233 ± 6 for $C_{37:2+37:3}$ in Englebrecht and Sachs (2005), 220 ± 16 for $C_{37:2+37:3}$ in Schouten et al. (2006), 198 ± 20 for $C_{37:3}$ and 180 ± 16 for $C_{37:2}$ in Wolhowe et al. (2009) than reported in this study in which we find $\varepsilon_{C37:3-water}$ of 180 ± 4 and $\varepsilon_{C37:2-water}$ of 158 ± 3 in water particles (Table 1). As coastal haptophytes are likely predominant in our samples, lower alkenone-water D/H fractionation (by up to 60‰ relative to Englebrecht and Sachs (2005)) suggests that coastal haptophytes may fractionate less than oceanic haptophytes.

4.2.2. Lack of co-variation between salinity and D/H fractionation in CB alkenones

The D/H fractionation between water and all four alkenones was invariant over the salinity range of 10–29 (Fig. 6A and Table 2). This result is at odds with three recent studies indicating a 1–3‰ decrease in D/H fractionation in lipids per unit increase in salinity (Schouten et al., 2006; Sachse and Sachs, 2008; Sachs and Schwab, 2011). In batch-cultured *E. huxleyi* and *G. oceanica* Schouten et al. (2006) observed a positive linear correlation between salinity and $\alpha_{alkenone-water}$, the slope of which implied a decrease in D/H fractionation in $C_{37:3} + C_{37:2}$ alkenones of 3.3‰ and 3.0‰, respectively, per unit increase of salinity over the salinity range 25–35. In the same CB sample set on which we report here we observed a 0.99‰ decrease in D/H fractionation in dinosterol (4α,23,24-trimethyl-5α-cholest-22E-en-3β-ol) per unit increase of salinity over the salinity range 10–29 (Sachs and Schwab, 2011). And in hypersaline ponds on Christmas Island in the central equatorial Pacific (Republic of Kiribati), a 0.8–1.1‰ decrease in D/H fractionation per unit increase in salinity was observed in phytene, n-C_{17} alkane and a mixture of total extractable lipids over the salinity range 35–150 (Sachse and Sachs, 2008). While the 3–4-fold higher sensitivity of D/H fractionation to salinity in Schouten et al. (2006)'s alkenones as compared to these other studies was likely due in (large) part to the associated changes in growth rate, there is strong evidence that D/H fractionation decreases in algal lipids in response to higher salinity.

We consider three hypotheses to explain the lack of co-variation between $\alpha_{alkenone-water}$ and salinity in the CB. (i) Growth rate and temperature changes cause D/H fractionation in alkenones that counteract the fractionation arising from salinity changes. (ii) The assemblage of alkenone-producing haptophytes changes along the Bay and each species has a different sensitivity to salinity, such that no apparent trend in $\alpha_{alkenone-water}$ occurs along the salinity gradient. (iii) Coastal haptophytes that likely predominate the assemblage of alkenone producers in the CB may have an enhanced osmoregulation capacity that circumvents the mechanisms that cause a change in alkenone–water D/H fractionation in response to salinity changes in other species of phytoplankton and cyanobacteria.

(i) Growth rate and temperature changes cause D/H fractionation in alkenones that counteract the fractionation arising from salinity changes. Culture and field studies have demonstrated that growth rate and temperature can influence D/H fractionation in lipids (Schouten et al., 2006; Wolhowe et al., 2009; Zhang et al., 2009), but the data are few and the results contradictory.Zhang et al. (2009) showed that acetogenic lipids (C_{14}; $C_{16:1}$; C_{16}; C_{18} fatty acids) from two species of freshwater green algae (*E. unicocca* and *V. aureus*) grown in batch culture at 15 °C were enriched in deuterium by 20–40‰ relative to those grown at 25 °C. Similarly, Wolhowe et al. (2009) observed that individual alkenones from batch-cultured *E. huxleyi* and *G. oceanica* at 17 °C were enriched in deuterium by 40–50‰ relative to those grown at 25 °C. However, Schouten et al. (2006) observed no significant effect of temperature on alkenone–water D/H fractionation in batch-cultured *E. huxleyi* and *G. oceanica*, but growth rate changed along with temperature in these experiments. In the CB, the lack of any trend between alkenone–water D/H fractionation and temperature also suggests that temperature was not a first order influence on individual alkenone δD values (Fig. 6B). Growth rate has also been shown to influence D/H fractionation. Schouten et al. (2006) observed a substantial increase in D/H fractionation as growth rate increased in batch-cultured *E. huxleyi* and *G. oceanica* in response to different temperatures and salinities. In continuous culture experiments (i.e., chemostats), Zhang et al. (2009) found that D/H fractionation also increased substantially as growth rate increased in a sterol from the diatom *T. pseudonana*, but little or not at all in fatty acids from the same cultures. Growth rate trends from other phytoplankton groups in the CB indicate highest values in the mid-Bay and lowest values near the mouth of the Bay (Xu and Hood, 2006), opposite to those required to counteract the expected decrease of alkenone-water D/H fractionation as salinity increases along the Bay.

(ii) The assemblage of alkenone-producing haptophytes changes along the Bay and each species has a different sensitivity to salinity, such that no apparent trend in $\alpha_{alkenone-water}$ occurs along the salinity gradient. Different species of alkenone producers and other phytoplankton are known to produce the same lipids with different δD values when grown in water with the same salinity (cf., Schouten et al., 2006) or in water with the same δD value (e.g., Zhang and Sachs,

2007). Schouten et al. (2006) demonstrated that D/H fractionation in alkenones from *E. huxleyi* and *G. oceanica* grown in water with the same salinity differed by about 30‰. Though we know of no study reporting D/H fractionation in alkenones from coastal species such as *C. lamellosa* and *I. galbana*, it seems reasonable to assume that they too fractionate hydrogen differently, and consequently that a change in the assemblage of alkenone producing haptophytes along the Bay influenced $\alpha_{alkenone-water}$.

(iii) Coastal haptophytes that likely predominate the assemblage of alkenone producers in the CB may have an enhanced osmoregulation capacity that circumvents the mechanisms that cause a change in alkenone–water D/H fractionation in response to salinity changes in other species of phytoplankton and cyanobacteria. The observation that D/H fractionation in dinosterol of the CB dinoflagellates diminished as salinity increased (Sachs and Schwab, 2011), but remained constant in alkenones of the CB haptophytes, suggests that the effect of salinity on D/H fractionation in lipids is species dependant. Increasing salinity is particularly challenging for phytoplankton since lower water potential occurring during hyperosmotic stress reduces external water availability and increases harmful ion concentrations in the cell (Epstein, 1980). Sachse and Sachs (2008) and Sachs and Schwab (2011) proposed that algal lipid D-enrichment with increasing salinity results from the progressive D-enrichment of internal cell water as H is preferentially drawn from the internal water pool for biosynthetic reactions, and the flux of external water into the cell slows. Furthermore, since enzyme activities are affected by elevated cytoplasmic ion concentrations (Niu et al., 1995; Kirst, 1989) and ultimately control lipid δD values (Baillif et al., 2009; Chikaraishi et al., 2009; Schwab and Sachs, 2009), it is likely that elevated cytoplasmic ion concentrations occurring during hyperosmotic stress may hamper vital enzymes involved in lipid synthesis and their resultant δD values. As both cellular internal water volume and cytoplasmic ion concentration affect water potential during hyperosmotic stress (Haines, 1994; Jahnke and White, 2003), lipid δD values are expected to be affected by the capacity of algae to reduce water loss and internal concentrations of incompatible ions (i.e., osmoregulate). Conversely, at low external salinities the flux of external water into the cell increases and deleterious ion concentrations in the cytoplasm decrease. For instance, in the marine alga, *Dunaliella tertiolecta*, a high flux of external water into the cell under extreme hypoosmotic stress caused a larger cell volume and a higher concentration of α-tocopherol, indicative of heightened stress within the chloroplast membrane (Jahnke and White, 2003). Under this condition, the D/H ratio of the internal cell water is likely to be similar to the D/H ratio of the external water, resulting in lipid δD values that are more likely to reflect those of the environmental water. In CB, such hypo- and hyper-osmotic stress was probably not so intense, but the mechanisms that drove water flux into and out of the cell were likely similar.

4.3. Paleoenvironmental implications

The difference in sensitivity of D/H fractionation to salinity in CB haptophytes versus CB dinoflagellates indicates that salinity reconstructions based on paleo-lipid δD values may be species dependant. Some species may synthesize lipids with D/H ratios that are sensitive to salinity variations, others may synthesize lipids with δD values that are independent of salinity. The latter are likely to be good targets for water isotopic reconstructions.

Furthermore, the consistency of individual D/H fractionation factors between alkenones and water ($\alpha_{alkenone-water}$) in suspended particles and in sediment of the CB, and the similarity between slope- and intercept-derived fractionation factors (Table 2), suggest that water δD values are the primary control on changing alkenone δD values along the Bay and thus, CB water δD values may be determined using individual alkenone δD values with the equations listed in Table 1.

However, constant hydrogen isotope offsets between alkenones with different chain lengths but the same degree of unsaturation ($\alpha_{C37:2\text{-}C38:2}$ and $\alpha_{C37:3\ -\ C38:3} \approx 1.01$) and between those with the same chain length but different degrees of unsaturation ($\alpha_{C37:3\ -\ C37:2}$ and $\alpha_{C38:3\ -\ C38:2} \approx 0.97$) suggest that single, well-defined values represent hydrogen isotope fractionation associated with enzymatic dehydrogenation and carboxylation reactions during alkenone biosynthesis in the CB (Rontani et al., 2006; Chikaraishi et al., 2009; Schwab and Sachs, 2009). This observation strengthens the argument of Wolhowe et al. (2009) that these values may be used in isotopic mass balance calculations to determine δD values for individual alkenones without the labor intensive LC-MS separation developed by Schwab and Sachs (2009) and used in this study. However, further evaluation of the universality of the isotopic offset between different alkenones ought to be conducted in the lab and field before extending it to other coastal environments and corresponding species, since different salinity effects on $\alpha_{alkenone-water}$ in oceanic and coastal species suggest that physiological or morphological differences between alkenone producers may greatly influence alkenone δD values.

5. CONCLUSION

Alkenone distributions characterized by a high abundance of $C_{37:4}$ and high C_{37}/C_{38} ratios, in addition to the occurrence of uncalcified cells, support substantial contributions of coastal haptophyte species, such as *C. lamellosa* and *I. galbana*, in all studied surface sediment and suspended particle samples in the CB estuary.

The δD values of individual alkenones ($MeC_{37:2}$; $MeC_{37:3}$; $EtC_{38:2}$; $EtC_{38:3}$) closely co-varied with water δD values. Constant hydrogen isotope offsets ($\alpha_{C37:2\ -\ C38:2}$ and $\alpha_{C37:3\ -\ C38:3} = 1.01$ and $\alpha_{C37:2\ -\ C37:3}$ and $\alpha_{C38:2\ -\ C38} =$

0.97) were observed between the different alkenones in all studied samples along the Bay. This value was used in an isotopic mass balance calculation to determine δD values for individual alkenones in the CB when a mixture of two alkenones is analyzed (e.g., $C_{37:2} + C_{37:3}$)

Slope- and intercept- derived fractionation factors of the correlations ($\delta D_{alkenone} = \alpha_{alkenones-water}\delta D_{water} + \varepsilon$) describing the relationship between water and individual alkenone δD values did not differ significantly. No change in D/H fractionation ($\alpha_{alkenone-water}$) was observed along the salinity gradient of the Bay, suggesting that individual alkenone D/H ratios in the CB were primarily determined by source water δD values and that they may be used as proxy to reconstruct CB water δD values.

The difference in sensitivity of D/H fractionation to salinity in haptophytes relative to dinoflagellates in the CB indicates that the mechanisms of hydrogen isotope fractionation in different phytoplankton are influenced to a varying extent by salinity. By extension, paleosalinity reconstructions from lipid δD values are expected to be species dependant. Two valid hypotheses we consider to explain the lack of a salinity influence on alkenone-water D/H fractionation in the CB are: (i) the assemblage of alkenone-producing haptophytes changes along the Bay and each species has a different sensitivity to salinity, such that no apparent trend in $\alpha_{alkenone-water}$ occurs along the salinity gradient, and (ii) greater osmoregulation capacity in coastal haptophytes may result in little or no sensitivity of the D/H fractionation process during alkenone synthesis to salinity changes. Laboratory culture studies with oceanic, coastal and lacustrine alkenone-producing prymnesiophytes ought to provide a test of these hypotheses.

ACKNOWLEDGEMENTS

This material is based upon work supported by the National Science Foundation under Grants ESH-0639640, EAR-0745982 and EAR-0823503; the American Chemical Society through Petroleum Research Fund grant 46937-AC2; and by the Gary Comer Science and Education Foundation. The Swiss National Science Foundation is thanked for the postdoctoral fellowship accorded to V.F. Schwab. We are indebted to Rienk Smittenberg and Dirk Sachse for assistance in the field. We are grateful to Prof. Dr. P. Baumgartner for assistance with SEM analyses. We thank Prof. Dr. P. Baumgartner, Dr. P. Vonlanthen, Dr. P. Ziveri, Dr. M. Knappertsbusch and Dr. H. Kinkel for their help with species identifications. We thank Rienk Smittenberg, Orest Kawka, Dirk Sachse and Zhaohui Zhang for assistance in the laboratory. We also are grateful to the Virginia and Maryland monitoring programs for making their research vessels and facilities available to us, and to Rick Younger, captain of the R/V Kerhin from which many of the CB samples were collected. We thank Alex Sessions, two anonymous reviewers, and Associate Editor Jaap Sinninghe Damsté for their thoughtful comments that improved the manuscript.

APPENDIX A. SUPPLEMENTARY DATA

Supplementary data associated with this article can be found, in the online version, at doi:10.1016/j.gca.2011.09.031.

REFERENCES

Austin J. A. (2004) Estimating effective longitudinal dispersion in the Chesapeake Bay. *Estuar. Coast. Shelf Sci.* **60**, 359–368.

Baillif V., Robins R. J., Le Feunteun S., Lesot P. and Billault I. (2009) Investigation of fatty acids elongation and desaturation steps in *Fusarium lateritium* by quantitative two-dimensional deuterium NMR spectroscopy in chiral oriented media. *J. Biol. Chem.* **284**, 10783–10792.

Blanz T., Emeis K.-C. and Siegel H. (2005) Controls on alkenone unsaturation ratios along the salinity gradient between the open ocean and the Baltic Sea. *Geochim. Cosmochim. Acta* **69**, 3589–3600.

Brassell S. C., Eglington G., Marlowe I. T., Pfaumann U. and Sarnhein M. (1986) Molecular stratigraphy: a new tool for climatic assessment. *Nature* **320**, 129–133.

Chu G., Sun Q., Li S., Zheng M., Jia X., Lu C., Lu J. and Liu T. (2005) Long-chain alkenone distributions and temperature dependence in lacustrine surface sediments from China. *Geochim. Cosmochim. Acta* **69**, 4985–5003.

Chikaraishi Y., Tanaka R., Tanaky A. and Ohkouchi N. (2009) Fractionation of hydrogen isotope during phytol biosynthesis. *Org. Geochem.* **40**, 569–573.

Colman S. M. and Bratton J. F. (2003) Anthropogenically induced changes in sediment and biogenic silica fluxes in Chesapeake Bay. *Geology* **31**, 71–74.

Conte M. H., Volkman J. K. and Eglinton G. (1994) Lipids biomarkers of the Haptophyta. In *The Hapthophytes Algea* (eds. J. C. Green and B. S. C. Leadbeater). Oxford University Press, Oxford, UK, pp. 351–377.

Conte M. H., Thompson A. and Eglinton G. (1995) Lipid biomarker diversity in the coccolithophorid *Emiliania huxleyi* (Prymnesiophyceae) and the related species *Gephyrocapsa oceanica*. *J. Phycol.* **31**, 272–282.

Conte M. H., Thompson A., Lesley D. and Harris R. (1998) Genetic and physiological influences on the alkenone/alkenoates versus growth temperature relationship in *Emiliania huxleyi* and Gephyrocapsa Oceanica. *Geochim. Cosmochim. Acta* **62**, 51–68.

Coolen M. J. L., Muyzer G., Rijpstra W. I. C., Schouten S., Volkman J. K. and Damsté J. S. S. (2004) Combined DNA and lipid analyses of sediments reveal changes in Holocene haptophytes and diatoms population in an Antarctic lake. *Earth Planet. Sci. Lett.* **223**, 225–239.

Craig H. (1961) Isotopic variations in meteoric waters. *Science* **133**, 1702–1703.

Craig H. and Gordon L. (1965) Deuterium and oxygen 18 variations in the ocean and the marine atmosphere. In *Proceedings of a Conference on Stable Isotopes in Oceanographic Studies and Paleotemperatures* (ed. E. Tongiori). CNR-Laboratorio di Geologia Nucleare, Pisa.

Cranwell P. A. (1985) Long-chain unsaturated ketones in recent lacustrine sediments. *Geochim. Cosmochim. Acta* **49**, 1545–1551.

Cronin T. M., Hayo K., Thunell R. C., Dwyer G. S., Saenger C. and Willard D. A. (2010) The medieval climate anomaly and little ice age in Chesapeake Bay and the North Atlantic Ocean. *Palaeogeogr. Palaeoclimatol. Palaeoecol.* **297**, 299–310.

D'Andrea W. J., Liu Z., Da Rosa A. M., Wattley S., Herbert T. D. and Huang Y. (2007) An efficient method for isolating individual long-chain alkenones for compounds-specific hydrogen isotope analyses. *Anal. Chem.* **79**, 3430–3435.

Duan J. R., Billault I., Marbon F. and Robins R. (2002) Natural deuterium distribution in fatty acids isolated from peanut seed oil: a side-specific study by quantitative ^{2}H NMR spectroscopy. *ChemBioChem* **3**, 752–759.

Englebrecht A. C. and Sachs J. P. (2005) Determination of sediment provenance at drift sites using hydrogen isotopes and unsaturation ratios in alkenones. *Geochim. Cosmochim. Acta* **69**, 4253–4265.

Epstein E. (1980) Response of plants to saline environments. In *Genetic Engineering of Osmoregulation* (eds. D. W. Rains, R. C. Valentine and A. Hollaeander). Plenum Press, New York, pp. 7–21.

Green J. C., Course P. A. and Tarran G. A. (1996) The life-cycle of *Emiliania huxleyi*: a brief review and a study relative ploidy levels analyses by flow cytometry. *J. marine syst.* **9**, 33–44.

Haines T. H. (1994) Water transport across biological membranes. *FEBS Lett.* **346**, 115–122.

Herbert T. D. (2001) Review of alkenone calibrations (culture, water column, and sediments). *Geochem. Geophys. Geosyst.* **2**, 2000GC000055.

Huang Y., Shuman B., Wang Y. and Webb T. I. (2002) Hydrogen isotope ratios of palmitic acid in lacustrine sediments record late Quaternary climate variations. *Geology* **30**, 1103–1106.

Jahnke L. S. and White A. L. (2003) Long-term hyposaline and hypersaline stresses produce distinct antioxidant responses in the marine alga *Dunaliella tertiolecta*. *J. Plant Physiol.* **160**, 1193–1202.

Kreuzer-Martin H. W., Lott M. J., Ehleringer J. R. and Hegg A. L. (2006) Metabolic processes account for the majority of the intracellular water in log-phase *Escherichia coli* cells as revealed by hydrogen isotopes. *Biochemistry* **45**, 13622–13630.

Kirst G. O. (1989) Salinity tolerance of eukaryotic marine algae. *Annu. Rev. Plant Physiol. Mol. Biol.* **40**, 21–53.

Li J., Philp R. P., Pu F. and Allen J. (1996) Long-chain alkenones in Qinghai Lake sediments. *Geochim. Cosmochim. Acta* **60**, 235–241.

Marlowe I. T., Green J. C., Neal A. C., Brassell S. C., Eglinton G. and Course P. A. (1984) Long chain (n-C_{37-39}) alkenones in the Prymnesiophyceae. Distribution of alkenones and other lipids and their taxonomic significance. *Br. Phycol. J.* **19**, 203–216.

Marlowe I. T., Brassell S. C., Eglinton G. and Green J. C. (1990) Long chain alkenones and alkyl alkenoates and the fossil coccolith record of marine sediments. *Chem. Geol.* **88**, 349–375.

Marshall H. G. (1994) Chesapeake Bay phytoplankton: I. Composition. *Proc. Biol. Soc. Wash.* **107**, 573–585.

Marshall H. G., Burchardt L. and Lacouture R. (2005) A review of phytoplankton composition within Chesapeake Bay and its tidal estuaries. *J. Plankton Res.* **27**, 1083–1102.

Mercer J. L., Zhao M. and Colman S. M. (2005) Seasonal variations of alkenes and U^K_{37} in the Chesapeake Bay water column. *Estuar. Coast. Shelf Sci.* **63**, 675–682.

Niu X., Bressan R. A., Hasegawa P. M. and Pardo J. M. (1995) Ion homeostasis in NaCl stress environments. *Plants Physiol.* **109**, 735–742.

Paasche E. (2002) A review of the coccolithophorid *Emiliania huxleyi* (Prymnesiophyceae) with particular reference to growth, coccolith formation, and calcification-photosynthesis interactions. *Phycologia* **40**, 503–529.

Pahnke K., Sachs J. P., Keigwin L. D., Timmermann A. and Xie S.-P. (2007) Eastern tropical Pacific hydrologic changes during the past 27'000 years from D/H ratios in alkenones. *Paleoceanography* **22**, PA4214.

Prahl F. G. and Wakeham S. F. (1987) Calibration of unsaturation patterns in long-chain ketone composition for paleotemperature assessment. *Nature* **330**, 367–369.

Prahl F. G., Muchlhausen L. A. and Zahnle D. I. (1988) Further evaluation of long-chain alkenones as indicators of paleooceanographic conditions. *Geochim. Cosmochim. Acta* **52**, 2303–2310.

Pritchard D. W. (1967) What is an estuary, physical viewpoint. In *Estuaries* (ed. G. H. Lauff). American Association for the Advancement of Science, Washington, DC, publ. no. 83.

Rontani J.-F., Beker B. and Volkman J. K. (2004) Long-chain alkenones and related compounds in the benthic haptophyte *Chrysotila lamellosa* Anand HAP 17. *Phytochemistry* **65**, 117–126.

Rontani J.-F., Prahl F. G. and Volkman J. K. (2006) Re-examination of the double bond positions in alkenones and derivatives: biosynthetic implication. *J. Phycol.* **42**, 800–813.

Rosell-Melé A. (1998) Interhemispheric appraisal of the value of alkenone indices as temperature and salinity proxies in high-latitude location. *Paleoceanography* **13**, 694–703.

Sachs J. P. and Schwab V. F. (2011) Hydrogen isotopes in dinosterol from the Chesapeake Bay estuary. *Geochim. Cosmochim. Acta* **72**, 444–459.

Sachs J. P., Sachse D., Smittenberg R. H., Zhang Z., Battisti D. S. and Golubic S. (2009) Southward movement of the Pacific intertropical convergence zone AD 1400–1850. *Nat. Geosci.* **2**, 519–525.

Sachse D. and Sachs J. (2008) Inverse relationship between D/H fractionation in cyanobacterial lipids and salinity in Christmas Island saline ponds. *Geochim. Cosmochim. Acta* **72**, 793–806.

Sauer P. E., Eglinton T. I., Hayes J. M., Schimmelmann A. and Sessions A. L. (2001) Compound-specific D/H ratios of lipid biomarkers from sediments as a proxy for environmental and climatic conditions. *Geochim. Cosmochim. Acta* **65**, 213–222.

Schouten S., Ossebaar J., Schreiber K., Kienhuis M. V. M., Langer G., Benthien A. and Bijma J. (2006) The effect of temperature, salinity and growth rate on the stable hydrogen isotopic composition of long chain alkenones produced by *Emiliania Huxleyi* and *Gephyrocapsca Oceanica*. *Biogeosciences* **3**, 113–119.

Schulz H.-M., Schöner A. and Emeis K.-C. (2000) Long-chain alkenone patterns in the Baltic Sea-an ocean-freshwater transition. *Geochim. Cosmochim. Acta* **64**, 469–477.

Schwab V. F. and Sachs J. P. (2009) The measurement of D/H ratio in alkenones and their isotopic heterogeneity. *Org. Geochem.* **40**, 111–118.

Sessions A. L., Burgoyne T. W., Schimmelmann A. and Hayes J. M. (1999) Fractionation of hydrogen isotopes in lipid biosynthesis. *Org. Geochem.* **30**, 1193–1200.

Sessions A. L., Burgoyne T. W. and Hayes J. M. (2001) Correlation of H_3^+ contributions in hydrogen isotope ratio monitoring mass spectrometry. *Anal. Chem.* **73**, 192–199.

Smittenberg R., Saenger C., Dawson M. and Sachs J. P. (2011) Compound-specific D/H ratios of the marine lakes of Palau as proxies for West Pacific Warm Pool hydrologic variability. *Quat. Sci. Rev.* **30**, 921–933.

Sun A., Chu G., Liu G., Li S. and Wang X. (2007) Calibration of alkenone unsaturation index with growth temperature for lacustrine species, *Chrysotila lamellosa* (haptophyceae). *Org. Geochem.* **38**, 1226–1234.

Theroux S., D'Andrea W. J., Toney J., Amaral-Zettler L. and Huang Y. (2010) Phylogenetic diversity and evolutionary relatedness of alkenone-producing haptophyte algae in lakes: implications for continental paleotemperature reconstructions. *Earth Planet. Sci. Lett.* **300**, 311–320.

Thiel V., Jenisch A., Landmann G., Reimer A. and Michaelis W. (1997) Unusual distribution of long-chain alkenones and tetrahymanol from the highly alkaline Lake Van, Turkey. *Geochim. Cosmochim. Acta* **61**, 2053–2064.

Toney J. L., Huang Y., Fritz S. C., Baker P. A., Grimm E. and Nyren P. (2010) Climatic and environmental controls on the occurrence and distributions of long chain alkenones in lakes of the interior United States. *Geochim. Cosmochim. Acta* **74**, 1563–1578.

Van der Meer M. T. J., Bass M., Rijpstra I. C., Marino G., Rohling E. J., Sinninghe Damsté J. S. and Schouten S. (2007) Hydrogen isotopic compositions of long-chain alkenones record freshwater flooding of the Eastern Mediterranean at the onset of sapropel deposition. *Earth Planet. Sci. Lett.* **262**, 594–600.

Van der Meer M. T. J., Sangiorgi F., Baas M., Brinkhuis H., Sinninghe Damsté J. S. and Schouten S. (2008) Molecular isotopic and dinoflagellatte evidence for Late Holocene freshening of the Black Sea. *Earth Planet. Sci. Lett.* **267**, 426–434.

Versteegh G. J. M., Riegman R., de Leeuw J. W. and Jansen J. H. F. F. (2001) U values for *Isochrysis galbana* as a function of culture temperature, light intensity and nutrient concentrations. *Org. Geochem.* **32**, 785–794.

Volkman J. K., Eglinton G., Corner E. D. S. and Forsberg T. E. V. (1980) Long chain alkenes and alkenones in the marine coccolithophorid *Emiliania huxleyi*. *Phytochemistry* **19**, 2619–2622.

Volkman J. K., Burton H. R., Everitt D. A. and Allen D. I. (1988) Pigment and lipid compositions of algal and bacteria communities in Ace Lake, Vestfold Hills, Antartica. *Hydrobiologia* **165**, 41–57.

Volkman J. K., Barrett S. M., Blackburn S. I. and Sikes E. L. (1995) Alkenones in *Geophyrocapsa oceanica*: implications for studies of paleoclimate. *Geochim. Cosmochim. Acta* **59**, 513–520.

Wolhowe M. D., Prahl F. G., Probert I. and Maldonado M. (2009) Growth phase dependent hydrogen isotopic fractionation in alkenone-producing haptophytes. *Biogeosciences* **6**, 1681–1694.

Xu J. and Hood R. R. (2006) Modeling biogeochemical cycles in Chesapeake Bay with a coupled physical-biogeochemical model. *Estuar. Coast. Shelf Sci.* **69**, 19–46.

Zhang Z. and Sachs J. P. (2007) Hydrogen isotope fractionation in freshwater algae: 1. Variations among lipids and species. *Org. Geochem.* **38**, 582–608.

Zhang Z., Sachs J. P. and Marchetti A. (2009) Hydrogen isotope fractionation in freshwater and marine algae: II. Temperature and nitrogen limited growth effects. *Org. Geochem.* **40**, 428–439.

Associate editor: Jaap S. Sinninghe Damste